

Deep inside the pion. Reconciling QCD theory with data

A. P. Bakulev* and S. V. Mikhailov†

Bogoliubov Laboratory of Theoretical Physics, JINR, 141980 Dubna, Russia

N. G. Stefanis‡

*Institut für Theoretische Physik II,
Ruhr-Universität Bochum, D-44780 Bochum, Germany*

Dedicated to Prof. Klaus Goeke on the occasion of his 60th birthday.

Abstract

Recent developments in the QCD description of the pion structure are reviewed. The CLEO pion-photon transition data analysis favors a distribution amplitude for the pion that is double-humped but endpoint-suppressed. After a short outline of the derivation of this amplitude from QCD sum rules with nonlocal condensates, we present the fully fledged analysis of the CLEO data prefaced by predictions for the $F^{\gamma\rho\pi}$ form factor and commenting on the inherent theoretical uncertainties due to higher twists and NNLO perturbative corrections. We supplement our discussion by considering within QCD factorization theory, the electromagnetic pion form factor at NLO accuracy on one hand, and diffractive di-jets production on the other, comparing our predictions with the respective experimental data from JLab and the Fermilab E791 collaboration. In all cases, the agreement is impressive.

PACS numbers: 11.10.Hi, 12.38.Bx, 12.38.Cy, 13.40.Gp

*Electronic address: bakulev@thsun1.jinr.ru

†Electronic address: mikhs@thsun1.jinr.ru

‡Electronic address: stefanis@tp2.ruhr-uni-bochum.de

I. INTRODUCTION

Advances in theoretical science are mostly based on finding useful and compact descriptions of a phenomenon of interest. Understanding the nonperturbative dynamics of quarks and gluons inside the pion is a question too difficult to be addressed from first principles within QCD. In order to gain some insight into the nonperturbative physics of the QCD vacuum, the concept of nonlocal condensates was introduced [1, 2, 3].

In this framework, a simple and compact descriptor of the complex vacuum structure is provided by the average virtuality $\langle k_q^2 \rangle = \lambda_q^2$ of vacuum quarks, whose inverse λ_q^{-1} defines the correlation length of the scalar quark nonlocal condensate. The nonlocality parameter has been estimated using QCD sum rules [4] and lattice calculations [5]; just recently [6] it has been extracted from the data of the CLEO collaboration [7] on the pion-photon transition. One finds values in the range $\lambda_q^2 = \langle \bar{q} (ig \sigma_{\mu\nu} G^{\mu\nu}) q \rangle / (2\langle \bar{q}q \rangle) = (0.35 - 0.5) \text{ GeV}^2$ which pertain to a correlation length varying, respectively, between 0.33 fm and 0.28 fm, while the CLEO data favors the value $\lambda_q^2 = 0.4 \text{ GeV}^2$ [6] and a correlation length of about 0.31 fm.

Using QCD sum rules within this framework and a Gaussian ansatz with the single parameter λ_q^2 for the vacuum distributions, the pion distribution amplitude (DA) was first derived in [1, 8]. Later, this approach was refurbished and rectified [9], providing constraints on the first ten moments of the pion DA and an estimate for the inverse moment using an *independent* sum rule. With recourse to the fast decrease of the moment values with its number N , [10, 11], the Gegenbauer coefficients of the pion DA were calculated within uncertainty ranges and it was found that only the first two of them a_2 and a_4 are important; the rest are negligible [9, 11]. This gives us a handy tool to reconstruct the pion distribution amplitude [9] and calculate with it pion observables, like the pion-photon transition form factor $F_{\pi\gamma^*\gamma^*}(Q^2)$ [6, 12, 13] and the electromagnetic form factor $F_\pi(Q^2)$ [14]. Confronting this pion DA (in terms of the first two Gegenbauer coefficients) with the constraints extracted from the CLEO data [7] via a best-fit analysis [15], it was found [6, 12] that it is within the 1σ -error ellipse while the exclusion of the Chernyak-Zhitnitsky (CZ) [16] distribution amplitude at the 4σ level and of the asymptotic one at the 3σ level was reinforced.

II. NONLOCAL CONDENSATES AND THE PION DISTRIBUTION AMPLITUDE

The pion DA is a universal process-independent characteristic of the pion, explaining how the longitudinal momentum P is partitioned between its two valence partons quark (x) and antiquark ($\bar{x} = 1 - x$), this being a reflection of the underlying nonperturbative dynamics. To leading twist-2, one has

$$\langle 0 | \bar{d}(z)\gamma^\mu\gamma_5\mathcal{C}(z,0)u(0) | \pi(P) \rangle \Big|_{z^2=0} = if_\pi P^\mu \int_0^1 dx e^{ix(zP)} \varphi_\pi(x, \mu_0^2), \quad (1)$$

where $\mathcal{C}(0, z) = \mathcal{P} \exp[-ig_s \int_0^z t^\alpha A_\mu^\alpha(y) dy^\mu]$ is the path-ordered phase factor (the connector [17]) to preserve gauge invariance, f_π is the pion decay coupling, and the normalization is $\int_0^1 dx \varphi_\pi(x, \mu^2) = 1$.

To get a handle on the pion DA, the aim is to relate it with the nonperturbative QCD vacuum in terms of nonlocal condensates. This is achieved by relating the pion and its first

resonance by means of a sum rule, based on the correlator of two axial currents:

$$f_\pi^2 \varphi_\pi(x) + f_{A_1}^2 \varphi_{A_1}(x) \exp\left(-\frac{m_{A_1}^2}{M^2}\right) = \int_0^{s_\pi^0} \rho_{\text{NLO}}^{\text{pert}}(x; s) e^{-s/M^2} ds + \frac{\langle \alpha_s GG \rangle}{24\pi M^2} \Phi_G(x; M^2) + \frac{8\pi\alpha_s \langle \bar{q}q \rangle^2}{81M^4} \sum_{i=S,V,T_{1,2,3}} \Phi_i(x; M^2). \quad (2)$$

Here the index i runs over scalar (S), vector (V), and tensor (T) condensates, M^2 is the Borel parameter, and s_π^0 is the duality interval in the axial channel, whereas $\rho_{\text{NLO}}^{\text{pert}}(x; s)$ is the spectral density in NLO perturbation theory [8, 9]. Above, the dependence on the crucial non-locality parameter λ_q^2 enters the sum rule in the way exemplified by the numerically important scalar-condensate contribution

$$\Phi_S(x; M^2) = \frac{18}{\Delta \Delta^2} \left\{ \theta(\bar{x} > \Delta > x) \bar{x} [x + (\Delta - x) \ln(\bar{x})] + (\bar{x} \rightarrow x) + \theta(1 > \Delta) \theta(\Delta > x > \bar{\Delta}) [\bar{\Delta} + (\Delta - 2\bar{x}x) \ln(\Delta)] \right\} \quad (3)$$

with $\Delta \equiv \lambda_q^2/(2M^2)$, $\bar{\Delta} \equiv 1 - \Delta$. One appreciates from this last expression that neglecting the vacuum correlation length (as in the approach of [16]), the end-point contributions ($x \rightarrow 0$ or 1) are strongly enhanced by $\delta(x), \delta'(x) \dots$ because for $\lambda_q^2 \rightarrow 0$ one obtains $\lim_{\Delta \rightarrow 0} \Phi_S(x; M^2) = 9[\delta(x) + \delta(1-x)]$. By virtue of the finiteness of λ_q^2 , the sum rule (2) can supply us with constraints on the first ten moments $\langle \xi^N \rangle_\pi \equiv \int_0^1 \varphi_\pi(x) (2x-1)^N dx$ of the pion DA that are decreasing with increasing polynomial order to zero, i.e., $\langle \xi^N \rangle \rightarrow [3/(N+1)(N+3)]$ (see Fig. 1 (a)). In addition, we can obtain an *independent* sum rule to constraint also the inverse moment $\langle x^{-1} \rangle_\pi \equiv \int_0^1 \varphi_\pi(x) x^{-1} dx$ quite accurately [9, 10] – see Fig. 1 (a). This is qualitatively how one derives correlated values of the first two Gegenbauer coefficients a_2 and a_4 in the (nonlocal) QCD sum-rules picture, given that the higher ones are practically zero (see Fig. 1 (b)). The final step is then to model the pion DA according to the expression

$$\varphi^{\text{BMS}}(x; \mu_0^2) = \varphi^{\text{as}}(x) \left[1 + a_2(\mu_0^2) C_2^{3/2}(2x-1) + a_4(\mu_0^2) C_4^{3/2}(2x-1) \right], \quad (4)$$

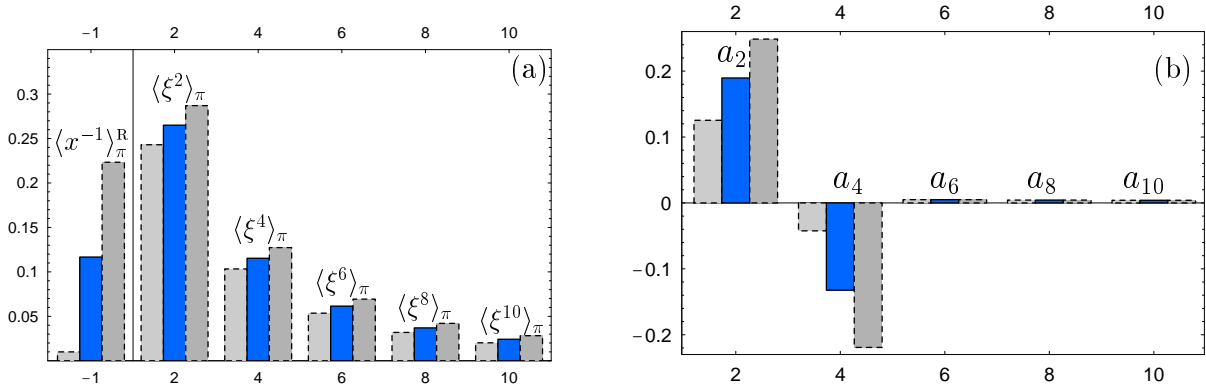


FIG. 1: (a) First ten ($N = 10$) nonzero moments, determined with nonlocal QCD sum rules [9], $\langle \xi^N \rangle_\pi$ and $\langle x^{-1} \rangle_\pi^{\text{R}} = (1/3)\langle x^{-1} \rangle_\pi - 1$ (the superscript R meaning “reduced”) of φ_{BMS} (dark blue bars) together with their upper and lower error-bars as light-grey bars. (b) Histogram of the first nonzero Gegenbauer coefficients a_n of the BMS pion DA and the envelopes of the “bunch” as light-grey bars.

providing the “bunch” of DAs shown in Fig. 2 (Left) together with the optimum sample, termed BMS model [9] ($a_2(\mu_0^2) = 0.2$, $a_4(\mu_0^2) = -0.14$), in comparison with the CZ and asymptotic pion DAs. Note that all DAs mentioned are normalized at the same scale $\mu_0^2 \simeq 1 \text{ GeV}^2$. In Table I, we compile the main features of our SRs, contrasting them with previous ones.

TABLE I: Determining the pion DA from QCD nonlocal sum rules, explaining the entries on its theoretical and phenomenological side, as well as its outcome. The differences between our present approach [9] and previous ones is pointed out.

Ref.	SR theor. part	SR phenom. part	SR estimates	Outcome
[1]	$O(\alpha_s)$ pQCD; quark, quark-gluon and gluon NLCs	π -state + continuum at $s_0 \approx 0.7 \text{ GeV}^2$	$\langle \xi^2 \rangle_\pi$, $\langle \xi^4 \rangle_\pi$, $\langle \xi^6 \rangle_\pi$	Pion DA should be closer to asymptotic rather than to CZ DA
[8]	[1] + modified gluon NLC	π - and A_1 -states + continuum at $s_0 \approx 2.2 \text{ GeV}^2$	$\langle \xi^2 \rangle_{\pi, A_1}, \dots, \langle \xi^{10} \rangle_{\pi, A_1}$, $\langle 1/x \rangle_{\pi, A_1}$ with error-bars	Two models of pion DAs: one includes the second Gegenbauer harmonic, i.e., $a_2 \neq 0$; the other is endpoint suppressed as $(x\bar{x})^{2.3}$
[9]	[8] + corrected quark-gluon NLC T_1	The same as in [8]: Borel window [0.5, 2] GeV^2	$\langle \xi^2 \rangle_{\pi, A_1}, \dots, \langle \xi^{10} \rangle_{\pi, A_1}$, $\langle 1/x \rangle_{\pi, A_1}$ with more conservative error-bars	“Bunch” of self-consistent DAs (Fig. 2(Left)) with 2 Gegenbauer harmonics (Fig. 1(b))

III. LIGHT-CONE SUM-RULE PREDICTIONS FOR $F^{\gamma^* \rho \pi}$

The $F^{\gamma \rho \pi}$ form factor appears as an inevitable part of the $F^{\gamma \gamma^* \pi}$ transition form factor in a light-cone sum-rule (LCSR) calculation. The main advantage of this method is that one can calculate the form factor for sufficiently large photon virtualities to obtain the perturbative spectral density, and then analytically continue the result to the limit $q^2 \simeq 0$ using a dispersion relation. In this scheme, $F^{\gamma \rho \pi}$ expresses the “hadronic” content of the quasi on-shell photon $\gamma(q^2)$ involved in the process $\gamma^*(Q^2) \gamma(q^2) \rightarrow \pi^0$. This calculational approach has been proposed by Khodjamirian in [18] and $F^{\gamma \rho \pi}(Q^2)$ was computed at the LO level of the LCSRs.

The form factor $Q^4 F^{\gamma \rho \pi}(Q^2)$ obtained in this framework depends mainly on the *differential* pion characteristic $\frac{d}{dx} \varphi_\pi(x)|_{x=\epsilon}$, $\epsilon \sim \frac{s_\rho}{Q^2}$, in an ϵ -neighborhood of the origin. This feature is opposite to the case of the $Q^2 F^{\gamma \gamma^* \pi}(Q^2)$ form factor, which depends mainly on the inverse moment $\langle x^{-1} \rangle_\pi = \int_0^1 \varphi_\pi(x; \mu^2) x^{-1} dx$, i.e., on an *integral* pion characteristic [9, 12]. From this point of view, $Q^4 F^{\gamma \rho \pi}(Q^2)$ can provide complementary information on the pion DA and help discriminate among different pion DA models.

Our predictions for $Q^4 F^{\gamma \rho \pi}(Q^2)$, based on the BMS bunch, Fig. 2 (Left), and on a complete NLO calculation for the corresponding spectral density [6], are presented in Fig. 2

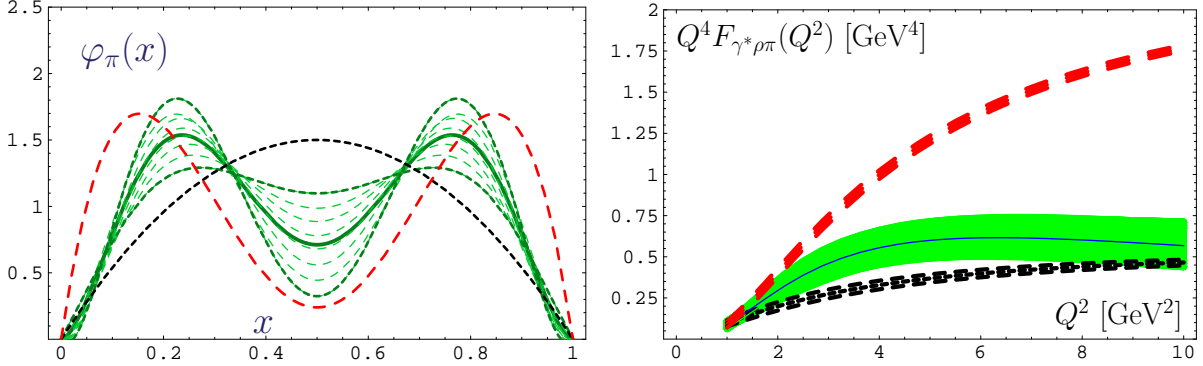


FIG. 2: **Left:** BMS “bunch” of the pion DAs contrasted with two extreme alternatives (asymptotic DA—dotted line and CZ model—long-dashed line) at $\mu^2 \approx 1 \text{ GeV}^2$. **Right:** Predictions for $Q^4 F_{\gamma^* \rho \pi}(Q^2)$ for the pion DAs shown on the left. The thickness of the two broken lines corresponds to the variation of the twist-4 parameter in the range $\delta_{\text{Tw-4}}^2 = (0.15 - 0.23) \text{ GeV}^2$.

(Right) in the form of a shaded strip, with the central line denoting the BMS model. These calculations are sketched in the next section. Here, let us mention only the main features: (i) The α_s -corrections appear to be rather large, of the order of 30%, and negative. (ii) The twist-4 contribution turns out to be very important, larger than 30% for Q^2 values below 3 GeV^2 and also negative. (iii) An improved Breit-Wigner ansatz for the phenomenological spectral density ρ^{mes} is used that increases the result for the form factor by about 6%.

Comparing the different models in Fig. 2 (Left), one can understand how the slope of $\varphi_\pi(x)$ in the domain $x \sim s_\rho/(Q^2 + s_\rho) \approx 0.2$ (at $s_\rho = 1.5 \text{ GeV}^2$, $Q^2 \approx 6 \text{ GeV}^2$) translates into the curve for the corresponding $Q^4 F^{\gamma^* \rho \pi}(Q^2)$ form factor in Fig. 2 (Right). All predictions shown are “smeared” curves, their thickness being a practical measure for the allowed variation of the twist-4 parameter $\delta_{\text{Tw-4}}^2 = (0.15 - 0.23) \text{ GeV}^2$.

IV. ANALYSIS OF THE CLEO DATA

Foremost among the many open questions in the nonperturbative regime of QCD is the determination of the parameters to model the shape of hadron DAs—prime examples being the pion Gegenbauer coefficients, on focus here, and those for the nucleon DA (for a review on the latter, see [19]). This task, though obviously of paramount importance is noted for its intransigence. However, the high-precision CLEO data [7] on the $\pi\gamma$ transition have improved the situation for the pion significantly.

Indeed, Schmedding and Yakovlev (SY) [15] have analyzed this data set using a further extension to the NLO (of pQCD) of the LCSR for the transition form factor $F^{\gamma^* \gamma \pi}(Q^2, q^2 \approx 0)$, developed in [18]. We adopted this approach in [6, 12] improving it in the following respects: (i) A more accurate point-to-point 2-loop ERBL [25] evolution has been employed, taking into account the quark thresholds. (ii) The contribution of the twist-4 term has been re-estimated to read $\delta^2(1\text{GeV}^2) = (0.19 \pm 0.02) \text{ GeV}^2$ and the role of these uncertainties has been investigated in detail. (iii) The procedure to determine the error range of the 1σ - and 2σ error contours has been improved and uncertainties of high-order radiative corrections have been involved in the analysis. For more detailed information and explicit expressions, the interested reader may consult [6, 12]. In the present exposition we take the opportunity

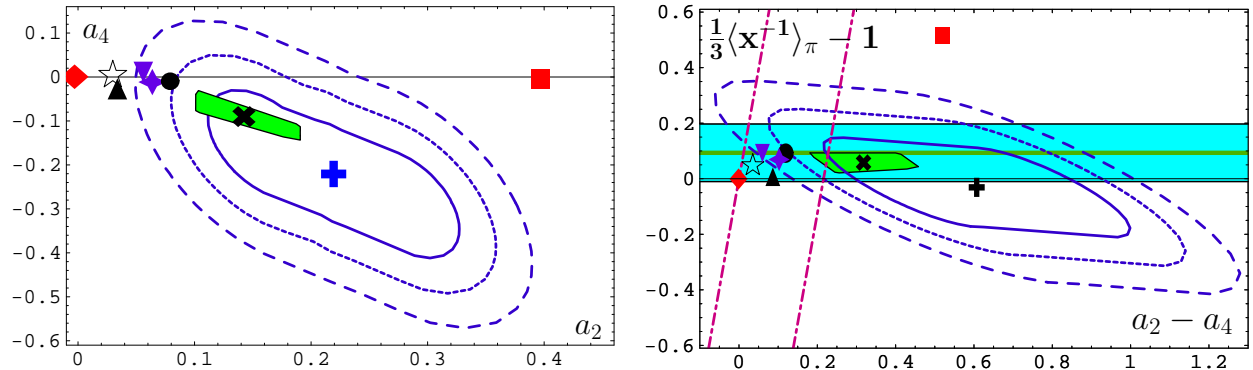


FIG. 3: **Left:** Analysis of the CLEO data on $F_{\pi\gamma^*\gamma}(Q^2)$ in the (a_2, a_4) plane in terms of error regions around the best-fit point, using for both panels the following designations: 1σ (solid line); 2σ (dashed line); 3σ (broken line). Various theoretical models are shown: \blacklozenge —asymptotic DA, \blacktimes —BMS model, \blacksquare —CZ DA, \blackplus —best-fit point, \star [20], \blacklozenge [21], \blacktriangle [22]—instanton models, \bullet [23]—Ball-Zwicky (BZ) model [23], and \blacktriangledown —transverse lattice result [24]. The slanted green rectangle represents the BMS “bunch” of pion DAs dictated by the nonlocal QCD sum rules for the value $\lambda_q^2 = 0.4 \text{ GeV}^2$. All constraints are evaluated at $\mu^2 = 5.76 \text{ GeV}^2$ after NLO ERBL evolution. **Right:** Results of the CLEO- data processing for $\langle x^{-1} \rangle_\pi^{\text{exp}}/3 - 1$ at $\mu_0^2 \approx 1 \text{ GeV}^2$ against theoretical predictions from QCD sum rules – hatched horizontal strip. The notations are the same as in the left panel.

to include in our graphics (see Fig. 3) the recent results of [23] (\bullet) and further extend our discussion of constraints on the Gegenbauer coefficients.

Let us summarize the main findings of our analysis taking recourse to figures 3. (i) The asymptotic DA and the CZ model are excluded at 3σ and 4σ , respectively—as pointed out before by SY in [15]. Several other proposed model DAs, extracted, for instance, from instanton-based approaches [20, 21, 22], or from lattice calculations [24] are also disfavored—at least at the level of 2σ , with the recently proposed model by Ball and Zwicky [23] lying exactly on the boundary of the 2σ error “ellipse”. The important observation here is that only the BMS “bunch” lies entirely inside the 1σ error area of the CLEO data. A similar picture arises also for the inverse moment $\langle x^{-1} \rangle_\pi^{\text{exp}}/3 - 1$ (right side of Fig. 3). The light solid line inside the hatched band indicates the mean value of the SR estimate, $\langle x^{-1} \rangle_\pi^{\text{SR}}/3 - 1 = 0.09$, and its error bars correspondingly. The strip bounded by two almost vertical dash-dotted lines corresponds to the rather old Braun–Filyanov [26] constraints: $\varphi_\pi(1/2; \mu_0^2) = 1.2 \pm 0.3$. (ii) The extracted parameters a_2 and a_4 were found to be rather sensitive to the strong radiative corrections and to the size of the twist-4 contribution. Nevertheless, even assuming a twist-4 uncertainty of the order of 30%, does not change these findings qualitatively. Still, both φ_{asy} and φ_{CZ} are outside the 3σ region with a slight improvement for the other models from 3σ to 2σ . (iii) The correlation length in the QCD vacuum was extracted directly from the CLEO data [6] and found to be $\Lambda \sim 0.31 \text{ fm}$, i.e., $\lambda_q^2 \lesssim 0.4 \text{ GeV}^2$. The prediction for the pion-photon transition form factor emerging from this analysis is shown in Fig. 4. The left-hand side shows the result for the twist-4 parameter $\delta_{\text{Tw-4}}^2 = 0.19 \text{ GeV}^2$, while the right-hand side illustrates the influence on the results of the variation of this parameter in the range $\delta_{\text{Tw-4}}^2 = (0.15 - 0.23) \text{ GeV}^2$. As one sees, in both cases, the prediction for the BMS “bunch” (shaded strip) is quite robust and in good agreement

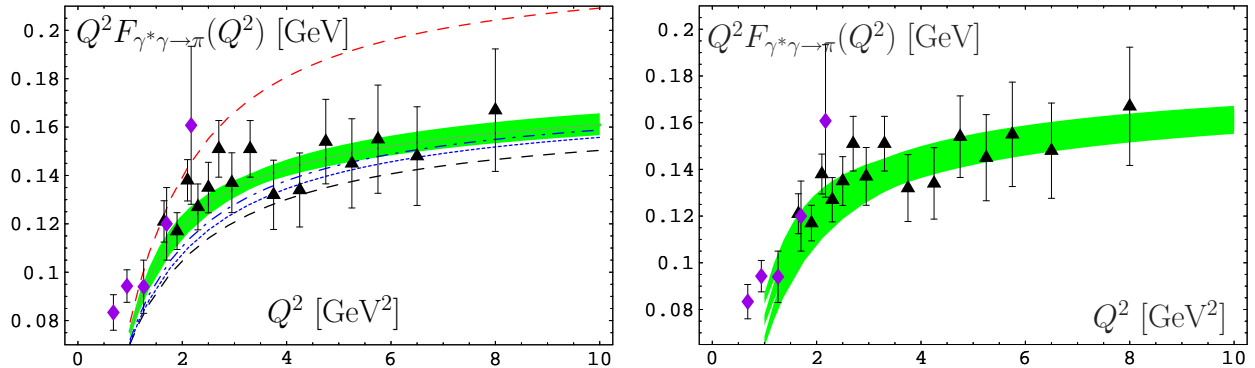


FIG. 4: **Left:** Light-cone sum-rule predictions for $Q^2 F_{\gamma^* \gamma \rightarrow \pi}(Q^2)$ in comparison with the CELLO (diamonds, [27]) and the CLEO (triangles, [7]) experimental data, evaluated with the twist-4 parameter value $\delta_{\text{Tw-4}}^2 = 0.19 \text{ GeV}^2$ [6, 12]. The predictions correspond to selected pion DAs; notably, φ_{CZ} (upper dashed line) [16], BMS-“bunch” (shaded strip) [9], two instanton-based models, viz., [20] (dotted line) and [21] (dash-dotted line), and φ_{as} (lower dashed line). **Right:** Similar predictions as in the left panel, but with the twist-4 parameter $\delta_{\text{Tw-4}}^2$ varied in the range $\delta_{\text{Tw-4}}^2 = 0.15 - 0.23 \text{ GeV}^2$.

with both sets of data—even at relatively low Q^2 values which exceed the validity of the theoretical framework applied.

V. PION’S ELECTROMAGNETIC FORM FACTOR

We have calculated in [14] the electromagnetic pion form factor

$$F_{\pi}(Q^2; \mu_R^2) = F_{\pi}^{\text{LD}}(Q^2) + F_{\pi}^{\text{Fact-WI}}(Q^2; \mu_R^2), \quad (5)$$

where the soft part $F_{\pi}^{\text{LD}}(Q^2)$ is modelled via local duality and the factorized contribution

$$F_{\pi}^{\text{Fact-WI}}(Q^2; \mu_R^2) = \left(\frac{Q^2}{2s_0^{2-\text{loop}} + Q^2} \right)^2 F_{\pi}^{\text{Fact}}(Q^2; \mu_R^2) \quad (6)$$

with $s_0^{2-\text{loop}} \simeq 0.6 \text{ GeV}^2$ has been corrected via a power-behaved pre-factor in order to respect the Ward identity at $Q^2 = 0$. In our analysis $F_{\pi}^{\text{Fact}}(Q^2; \mu_R^2)$ has been computed to NLO [28, 29], using Analytic Perturbation Theory [30, 31] and trading the running coupling and its powers for analytic expressions in a non-power series expansion, i.e.,

$$[F_{\pi}^{\text{Fact}}(Q^2; \mu_R^2)]_{\text{MaxAn}} = \bar{\alpha}_s^{(2)}(\mu_R^2) \mathcal{F}_{\pi}^{\text{LO}}(Q^2) + \frac{1}{\pi} \mathcal{A}_2^{(2)}(\mu_R^2) \mathcal{F}_{\pi}^{\text{NLO}}(Q^2; \mu_R^2), \quad (7)$$

with $\bar{\alpha}_s^{(2)}$ and $\mathcal{A}_2^{(2)}(\mu_R^2)$ being the 2-loop analytic images of $\alpha_s(Q^2)$ and $(\alpha_s(Q^2))^2$, correspondingly (see [14] and further references cited therein), whereas $\mathcal{F}_{\pi}^{\text{LO}}(Q^2)$ and $\mathcal{F}_{\pi}^{\text{NLO}}(Q^2; \mu_R^2)$ are the LO and NLO parts of the factorized form factor, respectively. The phenomenological upshot of this analysis is presented in Fig. 5(a), where we show $F_{\pi}(Q^2)$ for the BMS “bunch” and using the “Maximally Analytic” procedure, which improves the previously introduced [32] “Naive Analytic” one. This new procedure replaces the running coupling and its powers by their analytic versions, each with its own dispersive image [30, 31] and provides results

in rather good agreement with the experimental data [33, 34], given also the large errors of the latter. One appreciates that the form-factor predictions are only slightly larger than those resulting with the asymptotic DA.

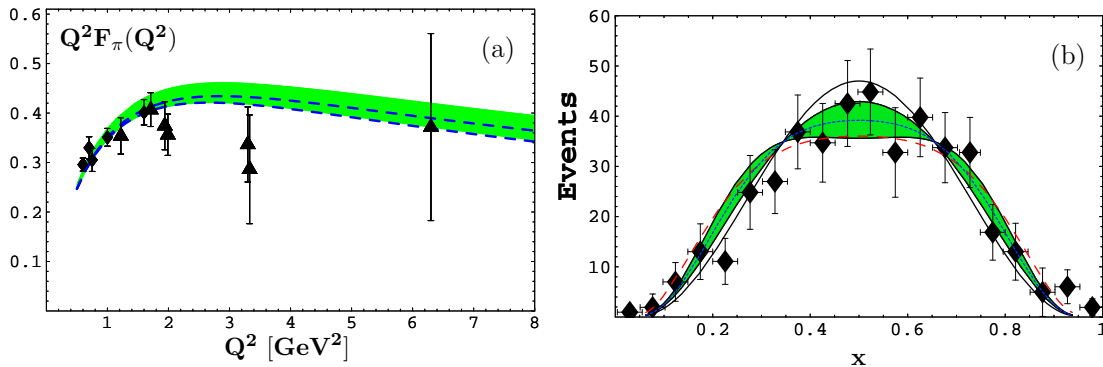


FIG. 5: (a) Predictions for the scaled pion form factor calculated with the BMS bunch (green strip) encompassing nonperturbative uncertainties from nonlocal QCD sum rules [9] and renormalization scheme and scale ambiguities at the level of the NLO accuracy. The dashed lines inside the strip restrict the area of predictions accessible to the asymptotic pion DA using the “Maximally Analytic” procedure [14]. The experimental data are taken from [34] (diamonds) and [33] (triangles). (b): Comparison with the E791 data [35] on diffractive di-jet production of the BMS “bunch” (shaded strip), the asymptotic DA (solid line), and the CZ (dashed line) model, using the convolution approach of [36].

VI. CONCLUSIONS

We have discussed pion DAs, derived from nonlocal QCD sum rules that implement the idea of a nonzero vacuum correlation length, and extracted for this latter quantity a value around ~ 0.31 fm directly from the CLEO data. The same set of experimental data offers the possibility to determine the Gegenbauer coefficients a_2 and a_4 within restricted error regions. Using a data processing, based on light-cone sum rules, we have shown that only the BMS-like pion DAs lie within the 1σ region, while all other known models are excluded at least at 2σ or more. We have given theoretical predictions for the electromagnetic form factor using NLO Analytic Perturbation Theory and shown that the same BMS “bunch” of pion DAs provides results very close to those obtained with the asymptotic DA. This agreement proves that whether or not the pion DA is double-humped or single-peaked is much less relevant compared to its endpoint behavior. In the BMS case, the root cause for the excellent agreement with the CLEO data is its strong endpoint suppression. These findings—gathered in Table II—are further backed up by the E791 data on diffractive di-jet production, albeit this set of data alone cannot favor one DA over the other. However, the fact that the middle region of x where the “bunch” has its largest uncertainties is within this data range, provides independent credibility for this type of pion DAs putting it into a wider general context. Finally, with the approved upgrade of the CEBAF accelerator at JLab, planned to provide precision data for the pion’s electromagnetic form factor up to $Q^2 = 6$ GeV², we expect that the confrontation between theory and experiment will make a decisive step forwards.

TABLE II: Pros and cons of selected pion DAs (asymptotic-like; BMS [9]; CZ [16]) in comparison with available experimental data.

π DA models	asymptotic-like	BMS [9]	CZ [16]
$\pi - \gamma$ CLEO data [7]	3σ off	within 1σ	4σ off
JLab F_π data [34, 37]	OK	OK	too large
Fermilab E791 [35]	$\chi^2 = 12.56$	$\chi^2 = 10.96$	$\chi^2 = 14.15$

Acknowledgments

It is a great pleasure to use this opportunity to wish Klaus Goeke to preserve his vigor and activity for the years to come. This work was supported in part by the Deutsche Forschungsgemeinschaft (436 RUS 113/752/0-1), the Heisenberg–Landau Programme (grants 2002 and 2003), the Russian Foundation for Fundamental Research (grants No. 03-02-16816 and 03-02-04022), and the INTAS-CALL 2000 N 587.

-
- [1] S. V. Mikhailov and A. V. Radyushkin, JETP Lett. **43**, 712 (1986); Sov. J. Nucl. Phys. **49**, 494 (1989); Phys. Rev. **D45**, 1754 (1992).
 - [2] A. P. Bakulev and A. V. Radyushkin, Phys. Lett. **B271**, 223 (1991).
 - [3] S. V. Mikhailov, Phys. Atom. Nucl. **56**, 650 (1993).
 - [4] V. M. Belyaev and B. L. Ioffe, Sov. Phys. JETP **57**, 716 (1983); A. A. Ovchinnikov and A. A. Pivovarov, Sov. J. Nucl. Phys. **48**, 721 (1988); A. A. Pivovarov, Bull. Lebedev Phys. Inst. **5**, 1 (1991).
 - [5] M. D’Elia, A. Di Giacomo, and E. Meggiolaro, Phys. Rev. **D59**, 054503 (1999); Nucl. Phys. Proc. Suppl. **83**, 512 (2000); A. P. Bakulev and S. V. Mikhailov, Phys. Rev. **D65**, 114511 (2002); Ting-Wai Chiu and Tung-Han Hsieh, Nucl. Phys. **B673** (2003) 217.
 - [6] A. P. Bakulev, S. V. Mikhailov, and N. G. Stefanis, Phys. Rev. **D67**, 074012 (2003).
 - [7] J. Gronberg et al. (CLEO), Phys. Rev. **D57**, 33 (1998).
 - [8] A. P. Bakulev and S. V. Mikhailov, Phys. Lett. **B436**, 351 (1998).
 - [9] A. P. Bakulev, S. V. Mikhailov, and N. G. Stefanis, Phys. Lett. **B508**, 279 (2001).
 - [10] A. P. Bakulev, S. V. Mikhailov, and N. G. Stefanis, in: Proceedings of the 36th Rencontres De Moriond On QCD And Hadronic Interactions, 17-24 Mar 2001, Les Arcs, France, edited by J. T. T. Van (World Scientific, Singapour, 2002), p. 133, hep-ph/0104290.
 - [11] A. P. Bakulev, S. V. Mikhailov, and N. G. Stefanis, in: Proceedings of the Light-Cone Workshop: Hadrons and Beyond (LC 03), Durham, England, 5-9 Aug 2003, edited by S. Dalley (Swansea), p. 172, hep-ph/0310267.
 - [12] A. P. Bakulev, S. V. Mikhailov, and N. G. Stefanis, Phys. Lett. **B578**, 91 (2004).
 - [13] A. P. Bakulev, S. V. Mikhailov, and N. G. Stefanis, hep-ph/0312141.
 - [14] A. P. Bakulev, K. Passek-Kumerički, W. Schroers, and N. G. Stefanis, Phys. Rev. **70**, 033014 (2004).
 - [15] A. Schmedding and O. Yakovlev, Phys. Rev. **D62**, 116002 (2000).
 - [16] V. L. Chernyak and A. R. Zhitnitsky, Phys. Rep. **112**, 173 (1984).
 - [17] N. G. Stefanis, Nuovo Cim. **A83**, 205 (1984).

- [18] A. Khodjamirian, Eur. Phys. J. C **6**, 477 (1999).
- [19] N. G. Stefanis, Eur. Phys. J. directC **1**, 7 (1999) [hep-ph/9911375].
- [20] V. Y. Petrov et al., Phys. Rev. **D59**, 114018 (1999).
- [21] M. Praszalowicz and A. Rostworowski, Phys. Rev. **D64**, 074003 (2001).
- [22] I. V. Anikin, A. E. Dorokhov, and L. Tomio, Phys. Part. Nucl. **31**, 509 (2000).
- [23] P. Ball and R. Zwicky, hep-ph/0406232; hep-ph/0406261.
- [24] S. Dalley and B. van de Sande, hep-ph/0212086.
- [25] A. V. Efremov and A. V. Radyushkin, Phys. Lett. **B94**, 245 (1980); Theor. Math. Phys. **42**, 97 (1980); G. P. Lepage and S. J. Brodsky, Phys. Lett. **B87**, 359 (1979); Phys. Rev. **D22**, 2157 (1980).
- [26] V. M. Braun and I. E. Filyanov, Z. Phys. **C44**, 1989, 157.
- [27] H. J. Behrend et al., Z. Phys. **C49**, 401 (1991).
- [28] B. Melić, B. Nižić and K. Passek, Phys. Rev. **D60**, 074004 (1999).
- [29] F. M. Dittes and A. V. Radyushkin, Sov. J. Nucl. Phys. **34**, 293 (1981); R. D. Field, R. Gupta, S. Otto and L. Chang Nucl. Phys. **B186**, 429 (1981); A. V. Radyushkin and R. S. Khalmuradov, Sov. J. Nucl. Phys. **42**, 289 (1985); E. Braaten and S.-M. Tse, Phys. Rev. **D35**, 2255 (1987).
- [30] D. V. Shirkov, hep-ph/0003242; Theor. Math. Phys. **127**, 409 (2001); *ibid.* **132**, 1309 (2002); Eur. Phys. J. **C22**, 331 (2001).
- [31] D. V. Shirkov and I. L. Solovtsov, Phys. Part. Nucl. **32S1**, 48 (2001).
- [32] N. G. Stefanis, W. Schroers, and H. C. Kim, Phys. Lett. **B449**, 299 (1999); Eur. Phys. J. **C18**, 137 (2000).
- [33] C. N. Brown et al., Phys. Rev. **D8**, 92 (1973); C.J. Bebek et al., **D13**, 25 (1976).
- [34] J. Volmer et al. (The Jefferson Lab F(pi)), Phys. Rev. Lett. **86**, 1713 (2001).
- [35] E. M. Aitala et al. (Fermilab E791), Phys. Rev. Lett. **86**, 4768 (2001).
- [36] V. M. Braun et al., Nucl. Phys. **B638**, 111 (2002).
- [37] H. P. Blok, G. M. Huber and D. J. Mack, nucl-ex/0208011.